

OVERVIEW OF SRF DEFLECTING AND CRABBING CAVITIES*

S. U. De Silva^{1†}, Old Dominion University, Norfolk, VA 23529, USA

Abstract

Developments over the past few years on novel superconducting deflecting and crabbing cavities have introduced advanced rf geometries with improved performance, in comparison to the typical squashed elliptical cavities operating in TM₁₁₀ type mode. These new structures are compact geometries operating in either TEM type or TE₁₁-like mode. One of the key applications of such cavities is the use of crabbing systems for circular colliders in increasing the luminosity. Crabbing systems are an essential component in future colliders with intense beams and proposed electron-ion colliders. High luminosity upgrade of LHC is planned to implement crabbings systems at two interaction points. Recently, a two-cavity cryomodule with double quarter wave crabbings cavity was installed in SPS at CERN and successfully tested with the proton beam. We present the details of different superconducting deflecting and crabbings cavities and their applications, as well as the recent results of the crabbings systems test at SPS.

INTRODUCTION

Superconducting deflecting and crabbings cavity design and development has seen tremendous progress due to the requirement with tight specifications on recent applications such as the LHC high luminosity upgrade [1] and future electron-ion colliders [2, 3]. These types of cavities are primarily used as deflecting cavities in separating a single beam into two or more beams, or as crabbings cavities in increasing the luminosity of particle colliders. In addition, these cavities are also used in emittance exchange of beams and in generating pulsed x-ray.

Concept of Deflecting Cavities

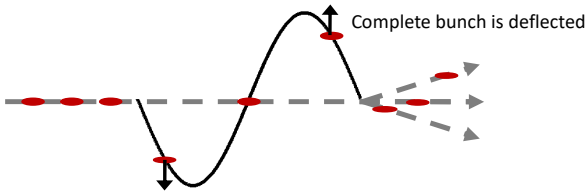


Figure 1: Deflecting cavities separate a single beam into multiple beams.

In deflecting cavities, the separation of single beam into multiple beams is achieved by applying a transverse voltage to the center of the bunch as shown in Fig. 1. The required transverse voltage is dependent on the beam energy (E_0) and the angle (θ) of separation required as given by

$$V_t = E_0 [eV] \theta [rad]. \quad (1)$$

*Work supported by DOE via US LARP Program and by the High Luminosity LHC Project and US DOE Award DE-SC0019149.

[†]sdesilva@jlab.org

Concept of Crabbing Cavities

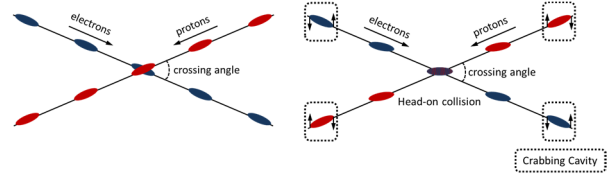


Figure 2: Bunch collision without (left) and with (right) crabbings cavities.

Luminosity increase in particle colliders requires maximizing the number of interactions between the colliding bunches. Non-overlapping bunches as shown in Fig. 2, limit the number of interactions due to crossing angle as given in

$$L = \frac{N_1 N_2 f_c N_b}{4\pi\sigma_x\sigma_y} \frac{1}{\sqrt{1 + \left(\frac{\sigma_z\theta_c}{2\sigma_x}\right)^2}} \quad (2)$$

where θ_c is the crossing angle. This limitation can be overcome by using crabbings cavities to enable head-on collision of bunches. The crabbings concept was first proposed by R.B. Palmer [4], in using a rf cavity to generate a transverse kick at the head and tail of the bunch that forces head-on collision at the interaction point of the colliding bunches as shown in Fig. 3. The required transverse kick for a crabbings cavity can be calculated as

$$V_t = \frac{cE_0 \tan\left(\frac{\varphi_{crab}}{2}\right)}{2\pi f_{rf} \sqrt{\beta_x^* \beta_c^c}} \quad (3)$$

where E_0 is the beam energy, φ_{crab} is the crossing angle, β_x^* is the betatron function at IP, β_c^* is the betatron function at the location of the crabbings cavity [5].

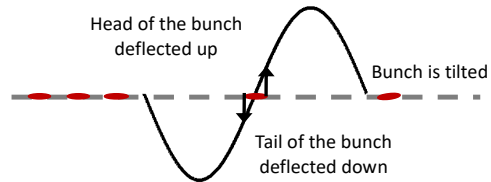


Figure 3: Applied transverse voltage in a crabbings cavity.

TYPES OF DEFLECTING AND CRABBING CAVITIES

Superconducting deflecting and crabbings cavities can be categorized in two 2 categories as

- i. TM₁₁₀-type cavities
- ii. TEM-type/TE₁₁-like cavities

based on the electromagnetic fields profile of the cavity geometry.

TM₁₁₀-Type Cavities

Cavities operating in TM₁₁₀ mode uses the transverse magnetic field interaction with the beam to generate transverse kick as shown in Fig. 4. The TM₁₁₀ mode is degenerate in a cylindrical-shaped geometry; therefore, a squashed-elliptical geometry is adapted to separate the two polarizations.

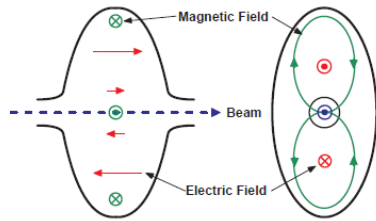


Figure 4: Squashed-elliptical crabbing cavity operating in TM₁₁₀ mode.

The squashed-elliptical cavity has a lower order mode (LOM), which is the TM₀₁₀ monopole mode present in the geometry. The narrow separation between the crabbing mode with LOM and HOMs while maintaining high R/Q for the crabbing mode makes the damping scheme very complex for these cavities. The operating frequency is inversely related to the transverse dimensions; hence these shapes are not favourable at low operating frequencies. At high operating frequencies TM₁₁₀-type cavities can deliver compact crabbing cavities that are capable of accommodating large beam apertures. The degrees of freedom in the parameter space for TM₁₁₀-type cavities are

limited, which makes the suppression of higher order multipole components difficult.

TEM-Type/TE₁₁-Like Cavities

In TEM-type or TE₁₁-like deflecting and crabbing cavities the primary contribution to the transverse kick is given by the transverse electric field as shown in Fig. 5. In pure cylindrical shaped TE-type cavities the net deflection from the magnetic field is cancelled by the net deflection from the electric field as stated in Panofsky-Wenzel theorem [6]. In order to generate a transverse deflection these cavities require deformed shapes.

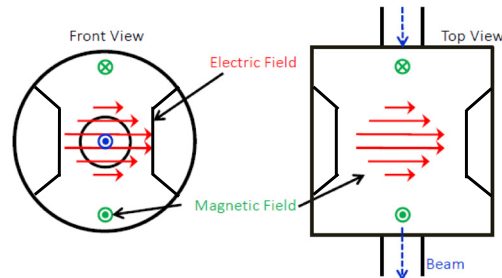


Figure 5: Cylindrical cavity with poles operating in TE₁₁-like mode.

TEM-type/TE₁₁-like cavities are compact designs that are favourable in low frequency operation. These designs also have high shunt impedance and low surface peak surface field ratios.

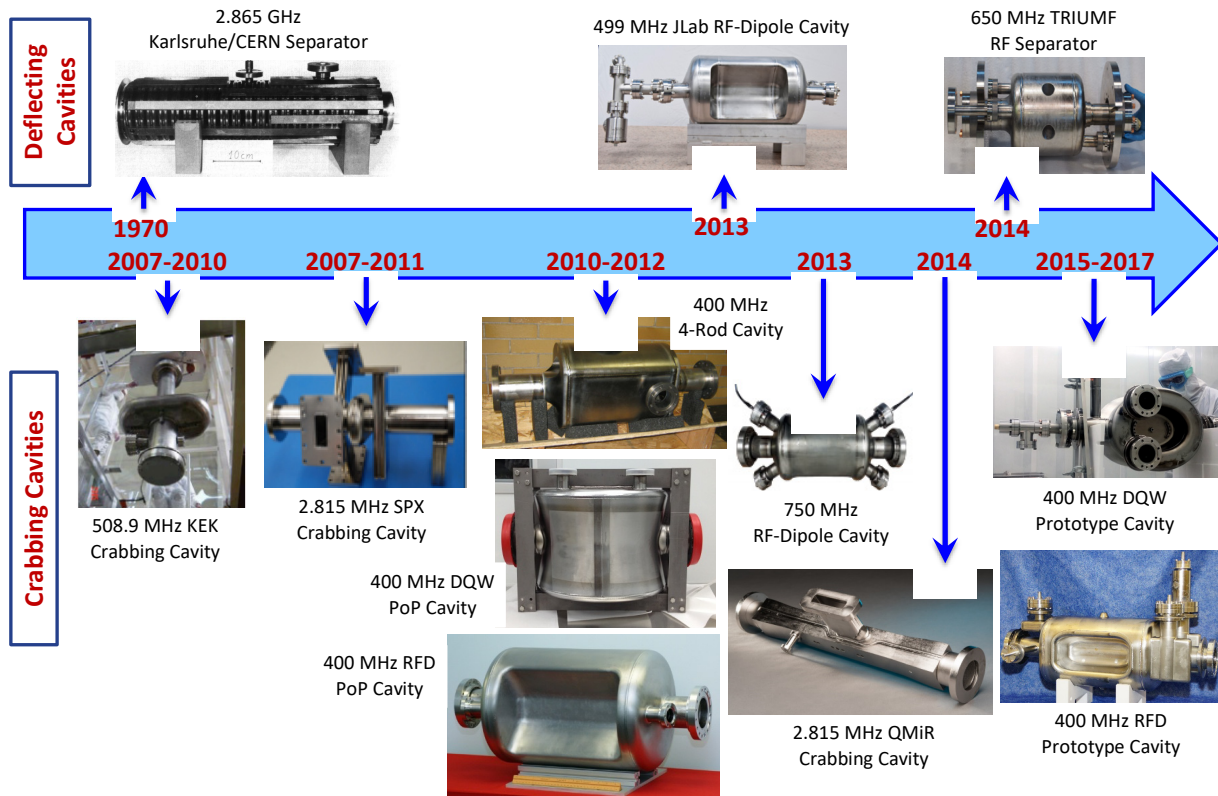


Figure 6: Sequence of superconducting deflecting and crabbing cavities that have been designed and fabricated.

EVOLUTION OF SUPERCONDUCTING DEFLECTING AND CRABBING CAVITIES

Over the years, a variety of superconducting deflecting and crabbing cavities have been designed, fabricated and tested at cryogenic temperatures. Figure 6 shows a timeline of such cavities designed for various deflecting and crabbing applications. In the early days, the common design of interest for deflecting and crabbing cavities was the cavities operating at TM_{110} mode with squashed elliptical geometry.

The 1st superconducting deflecting cavity was the 2.865 GHz rf separator with 104 cells operating in TM_{110} mode. The cavity was designed and fabricated at Karlsruhe and CERN in 1970s [7]. The rf separator was in operation from 1977 until 1981.

Similarly, the 1st superconducting crabbing cavity also operating in TM_{110} mode was designed around 1970 at KEK for the SuperB factory that was in operation from 2007 to 2010 [8]. The 508.9 MHz low operating frequency of the KEK crabbing cavity resulted in a large cavity with transverse dimensions of 866 mm and 483 mm. At the same time the 2.815 GHz crabbing cavity fabricated for the proposed short pulsed x-ray (SPX) project at ANL is a compact design operating in TM_{110} mode [9].

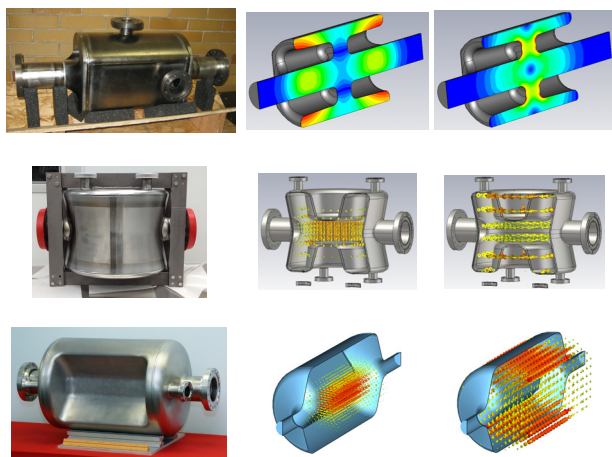


Figure 7: Proof-of-principle 4-rod cavity (top), double quarter wave cavity (centre), and rf-dipole cavity (bottom) with corresponding electric and magnetic field profiles.

Lately, the necessity of compact cavities operating at low frequencies for crabbing applications such as the LHC high luminosity upgrade and future electron ion colliders have led to the design of novel designs operating in either TEM mode or TE_{11} -like mode. Three such cavities are the 4-rod cavity [10], double quarter wave (DQW) cavity [11], and rf-dipole (RFD) cavity [12] that were initially proposed for the LHC high luminosity upgrade (HL-LHC). The fabricated proof-of-principle cavities are shown in Fig. 7. These cavities have successfully demonstrated the concept of rf designs, fabrication, processing, and rf performance.

The 2.815 GHz Quasi-waveguide Multicell Resonator (QMIR) shown in Fig. 6 is a crabbing cavity designed for

the proposed SPX project at ANL [13]. The QMIR cavity is a high frequency multi-cell cavity that operates in TE_{11} -like mode. The cavity diameter is designed to be of the size of the beam pipe aperture. The rf preformance of the fabricated cavity have demonstrated that these types cavities can be considered for high frequency applications [14].

APPLICATIONS OF DEFLECTING AND CRABBING CAVITIES

This section lists the recent work in the superconducting deflecting and crabbing applications.

TRIUMF RF-Separator

The deflecting cavity shown in Fig. 8 is a 650 MHz rf-separator cavity designed and fabricated for the TRIUMF ARIEL electron linac to split a single into two beams [15]. The transverse voltage requirement for the separator cavity is 0.3 MV. Due to the relaxed specification in the requirements the cavity was fabricated using reactor grade Nb with RRR 45. The cavity was machined out of a Nb block as shown in Fig. 8 and welded using Tungsten Inert Gas (TIG) welding as an alternative to electron beam welding.



Figure 8: Machined sub-assemblies (top) and fabricated (bottom) 650 MHz rf-separator.

The rf test results are shown in Fig. 9. The cavities achieved a transverse kick of 0.8 MV with $Q_0 > 2 \times 10^8$ exceeding the cavity specifications.

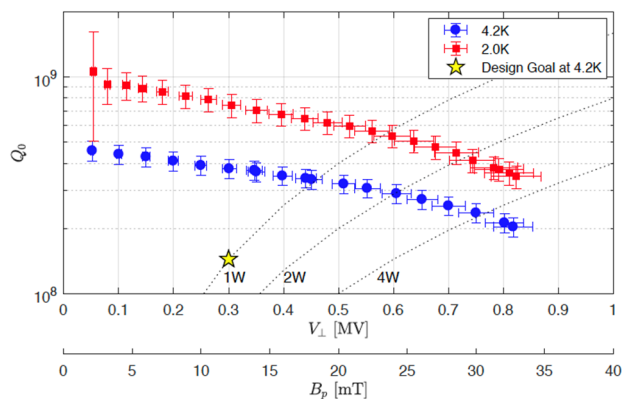


Figure 9: RF performance of the 650 MHz rf-separator cavity.

Crabbing Cavity Prototypes for HL-LHC

The HL-LHC upgrade requires two crabbing systems to be installed at the two interaction points of ATLAS and CMS. The DQW and RFD cavity types have been down selected for vertical crabbing and horizontal crabbing respectively [1]. The proof-of-principle cavities have been further optimized including the fundamental power coupler (FPC), HOM couplers, and field antenna as shown in Fig. 10. The DQW cavity design has 3 identical HOM couplers in addition, the pickup antenna also couples to one of the HOMs [16]. The RFD cavity has two HOM couplers named HHOM and VHOM that damps the horizontal dipole modes and vertical dipole modes respectively [17]. The rf properties listed in Table 1 shows that the two cavities operate at low peak surface fields at the nominal operating transverse voltage of 3.4 MV. Also, these geometries have no lower order modes with well separated HOMs from the fundamental operating mode.

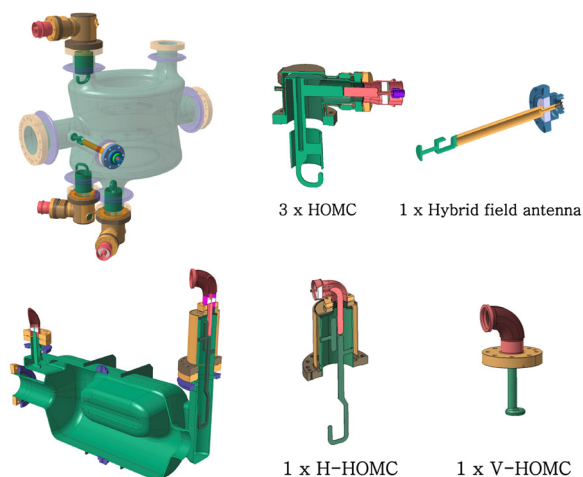


Figure 10: DQW (top) and RFD (bottom) crabbing cavity designs with HOM couplers.

Table 1: RF properties of the first prototypes of the DQW and RFD crabbing cavities shown in Fig. 10.

Parameter	DQW	RFD	Units
Frequency	400.79		MHz
LOM	None		MHz
Nearest HOM	567	633.5	MHz
V_T	3.4		MV
E_P	37.6	33	MV/m
B_P	72.8	56	mT
G	87	106.7	Ω
$[R/Q]_T$	429.3	429.7	Ω
$R_T R_S$	3.7×10^5	4.6×10^4	Ω^2

Two prototypes of each cavity have been fabricated and rf tested without and with HOM couplers to demonstrate the achievable performance of the complex cavities. The sub-assemblies were fabricated by Niowave Inc. and the final welds of all the 4 cavities were completed at Jefferson Lab followed by cavity processing and rf testing in house [18].

The cavity processing of both the cavities follows similar techniques used in processing elliptical cavities.

The summarized cavity processing and rf testing procedure followed by both the cavities are listed below.

- Bulk BCP
- Heat treatment at 600 °C for 10 hours
- Light BCP
- High pressure rinse
- Cavity assembly
- Low temperature bake at 120 °C
- Cavity rf test

The rf performance of the bare DQW cavity followed by the test results of the measurements of the cavity with a single HOM coupler are shown in Fig. 11 [19, 20]. The low field Q_0 was 9.8×10^9 where the Cavity 1 and 2 reached a maximum transverse voltage of 5.9 MV and 5.3 MV respectively at cryogenic temperature of 1.99 K. At nominal transverse voltage of 3.4 MV the power dissipation of both the cavities are less than 5 W.

The DQW Cavity 2 was followed up with further tests with a single HOM coupler installed on the cavity that was fabricated by CERN. The HOM coupler was processed following similar procedure carried out on the cavities, including bulk BCP, high temperature bake, and light BCP that improved the performance of the cavity rf test with HOM couplers as shown in Fig. 11(b). The cavity achieved a maximum transverse voltage of 4.7 MV and with a spacer installed to retract the HOM coupler further increased V_T to 5.1 MV.

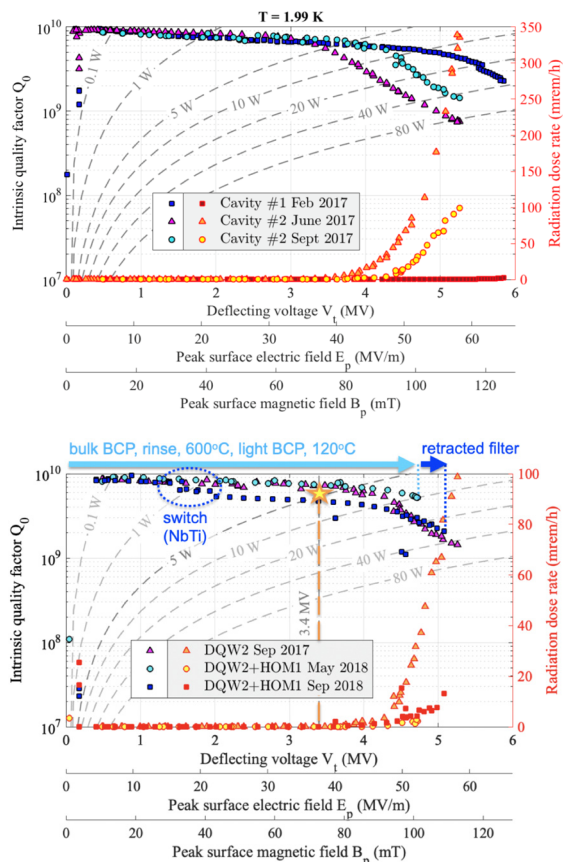


Figure 11: DQW bare cavity test (a-top) and test with a single HOM coupler (b-bottom).

Content from this work may be used under the terms of the CC BY 3.0 licence (© 2019). Any distribution of this work must maintain attribution to the author(s), title of the work, publisher, and DOI.

The rf performance of the bare RFD cavity is shown in the top plot in Fig. 12(a) [21]. The cavity achieved a maximum, transverse voltage of 5.8 MV with corresponding peak surface electric and magnetic fields of 56 MV/m and 95 mT. At nominal transverse voltage of 3.4 MV the power dissipation is 2.3 W.

One of the cavities was tested in identical test configuration with the two HOM couplers that was fabricated at Jefferson Lab. The demountable HHOM Nb coupler was processed with a light BCP and high pressure rinsed before installation. The rf performance shows similar results to that of the bare cavity with a maximum transverse voltage of 5.5 MV as shown in Fig 12(b). The slight drop in Q_0 resulted in a slightly higher power dissipation of 3.3 W.

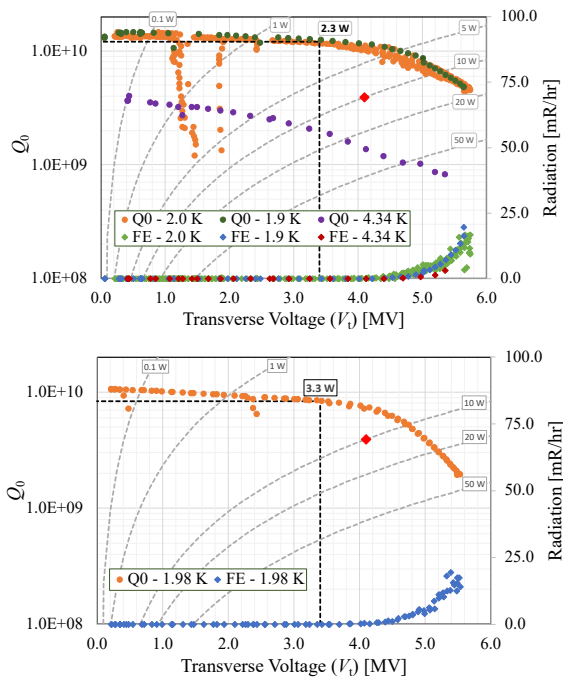


Figure 12: RFD bare cavity test (a-top) and test with HOM couplers (b-bottom).

The performance of both DQW and RFD cavities in rf tests have demonstrated that the cavities meet design specifications of transverse voltages exceeding 4.1 MV and power dissipation to be below 5 W at nominal voltage.

1ST CRABBING OF PROTON BEAMS

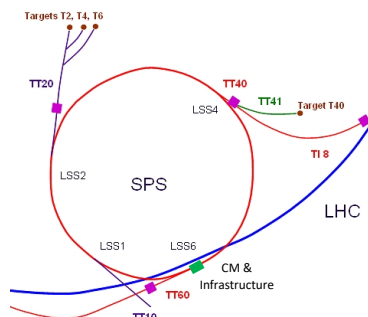


Figure 13: DQW-SPS cryomodule location on SPS.

The crabbing cavity system is an essential component in the HL-LHC upgrade. A two-cavity cryomodule with DQW crabbing cavities was installed in the SPS ring as shown in Fig. 13. This successfully demonstrated the 1st crabbing of a proton beam in a particle collider [22]. The SPS cryomodule program was completed in a short two-year program (2016-2018) from the fabrication of the cavities, cryomodule fabrication and installation to testing of the cryomodule with beam.

Figure 14 shows the installed cryomodule on the SPS beam line [23]. The cryomodule is installed on a moving table to allow regular operation of the SPS machine without interference from the crabbing cavities.



Figure 14: DQW cryomodule installed in SPS.

The two cavities installed on the SPS cryomodule were fabricated, processed and rf tested at CERN and the rf performance of the bare cavities are shown in Fig. 15 [24]. The cavities achieved design requirements of $V_t > 4.1$ MV at Q_0 corresponding to a dynamic heat load of 5 W.

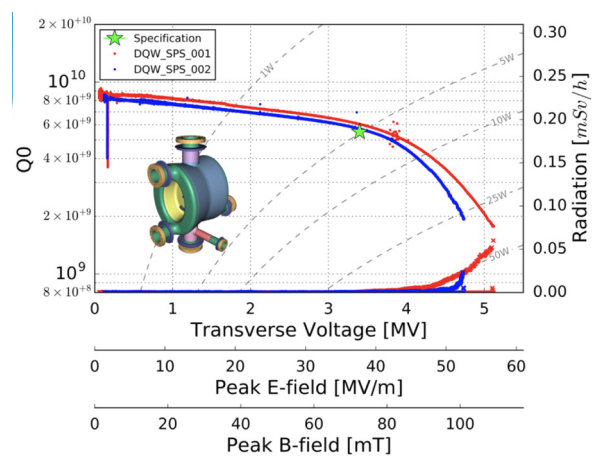


Figure 15: Bare cavity test results of the SPS-DQW cavities.

Figure 16 shows the detailed schematic of the SPS cryomodule with the DQW cavities with He vessels, cavity ancillaries, and tuning system, magnetic shielding, etc. [25]. The cryomodule was installed with a dedicated cryogenic system with a service module for liquid He supply and a refrigerator.

A sequence of 10 machine developments (MD) were allocated for the SPS beam test with the crabbing system [26] as listed in Table 2. The initial MDs were used in conditioning the cavities.

Table 2: Sequence of MDs Performed during SPS Cryomodule Test

MD#	Description	Cavity 1 [MV]	Cavity 2 [MV]	Temp [K]	Energy [GeV]
1	First crabbing, phase and voltage scan	0.5	0	4.5	26
2	270 GeV ramp with single bunch	1-2	0	4.5	26, 270
3	Intensity ramp up	1	~0.3	4.5	26
4	270 GeV coast setup	1.0	0.5	2.0	270
5	Emittance growth at 270 GeV with induced noise	0	1.0	2.0	270
6	Intensity ramp up to 4-batches	-	1.0-1.5	2.0	26
7	Intensity/Energy ramp up	-	1.0	2.0	26, 270, 400

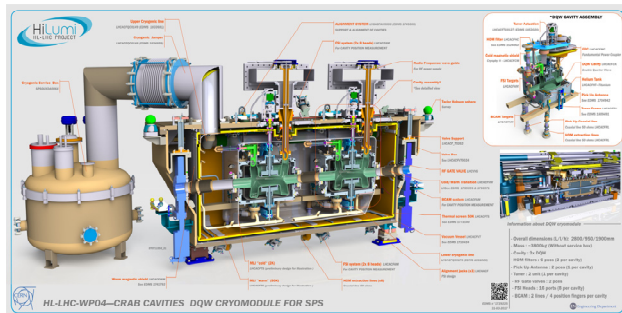


Figure 16: Schematic of DQW-SPS cryomodule.

The crabbing cavities were operated at 4.5 K in the initial MDs and after cavity conditioning the cavities were operated at 2.0 K. The MDs were planned to study the rf beam synchronization, transparency of the cavities to the beam, operation at high intensity and high energy [26]. The crabbing of the beam was observed by a head tail monitor as the main beam diagnostic method as shown in Fig. 17 [22]. The 1st crabbing of the proton beam was observed on May 23, 2018.

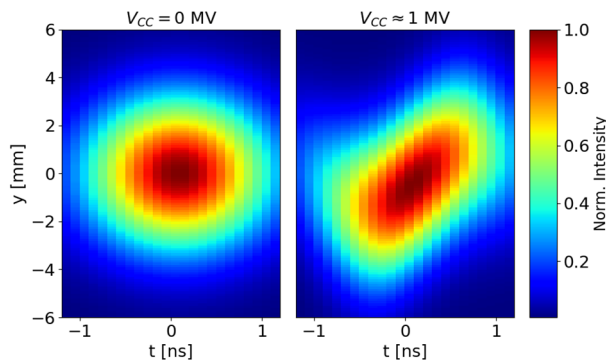


Figure 17: Crabbing voltage from the head-tail monitor [22].

The crabbing cavities also successfully demonstrated the transparency of the cavities to the beam. The two cavities in operation at 1 MV each in opposite phase cancels the net crabbing voltage with a residual kick of ~kV. The two cavities in phase resulted in a net transverse kick of 2 MV [22]. The lessons learned from the SPS cryomodule test are

being incorporated in both DQW and RFD crabbing cavity designs for the LHC cavity series production [27].

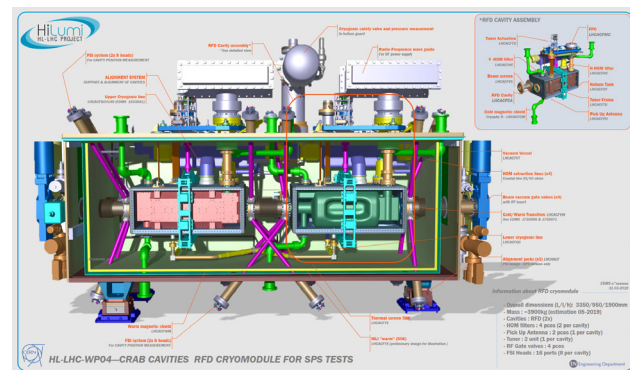


Figure 18: Schematic of RFD-SPS cryomodule.

Figure 18 shows the schematic of the RFD-SPS cryomodule design [28]. The cryomodule test is planned during year 2022. The prototype production of both DQW and RFD cavities for the LHC production series has been commissioned.

FUTURE ELECTRON-ION COLLIDERS

The future electron-ion colliders of eRHIC and JLEIC are proposed machines that requires crabbing cavity systems to increase the luminosity. The crabbing systems of these machine are critical component of the collider design in increasing luminosity compared to the HL-LHC upgrade. The corresponding beam parameters of the crabbing systems are listed in Table 3.

Table 3: Beam Parameters for eRHIC and JLEIC.

Parameter	eRHIC	JLEIC	Units
Frequency	338	952.6	MHz
Beam Energy (e/p)	10/275	12/200	GeV
Crossing Angle	22	50	mrad
V_r per beam per side (e/p)	4.0/13.0	4.2/21.5	MV

The crabbing cavity design proposed for the eRHIC is similar to that designed for LHC crabbing system with the an operating frequency of 338 MHz [29]. The crabbing cavity design for JLEIC will be a 2-cell RFD cavity design as shown in Fig. 19 operating at 952.6 MHz [30]. The large

Content from this work may be used under the terms of the CC BY 3.0 licence (© 2019). Any distribution of this work must maintain attribution to the author(s), title of the work, publisher, and DOI.

crossing angle requires a high net transverse voltage for both eRHIC and JLEIC.

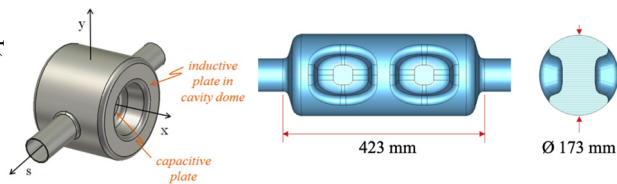


Figure 19: Crabbing cavity designs for eRHIC (left) and JLEIC (right).

CONCLUSION

The design and development of superconducting deflecting and crabbing cavities have evolved over the years from TM_{110} -type cavities to cavities operating in TEM-type or TE_{11} -like cavities. The recent applications of HL-LHC upgrade and future electron-ion colliders such as eRHIC and JLEIC require compact cavity designs that are capable of operating at low frequencies. The novel designs such as the double quarter wave cavity and rf-dipole cavity have many attractive properties such as low peak field ratios, high shunt impedance and no lower order modes present in the cavity. Furthermore, the successful rf tests carried out on prototype cavities shows the feasibility of operation at high transverse voltages with low power dissipation. The promising work has led to the successful implementation and operation of a superconducting crabbing cavity on a proton beam at the SPS in CERN.

ACKNOWLEDGEMENT

We would like to thank Niowave Inc. for providing the cavities and JLab SRF Institute for completing the fabrication, processing and rf testing of the cavities. We are grateful for the contributions in this field of work by CERN Work Package 4 (WP4), Cockcroft Institute and STFC in UK, Fermilab, BNL, SLAC, ODU, JLab, ANL and TRIUMF.

REFERENCES

- [1] G. Apollinari *et al.*, “High Luminosity Large Hadron Collider HL-LHC”, CERN Yellow Report, p. 19, May 2017.
- [2] C. Montag *et al.*, in *Proc. IPAC’19*, Melbourne, Australia, 2019, p. 45.
- [3] Y. Zhang, in *Proc. IPAC’19*, Melbourne, Australia, 2019, p. 1916.
- [4] R. B. Palmer, “Energy Scaling, Crab Crossing and the Pair Problem”, SLAC-PUB-4707, 1988.
- [5] Y.-P. Sun *et al.*, *Phys. Rev. Accel. Beams*, vol. 12, p. 101002, 2009.
- [6] W. K. H. Panofsky, W. A. Wenzel, *Rev. Sci. Instrum.*, vol. 27, p. 967, 1956.
- [7] A. Citron *et al.*, *Nucl. Instr. Meth.*, vol. 164, p. 31, 1979.
- [8] K. Hosoyama *et al.*, in *Proc. SRF’95*, Gif-sur-Yvette, France, p. 671.
- [9] H. Wang, “SPX Crab Cavity Development and Testing Result”, TTC Meeting, 2012.
- [10] B. Hall *et al.*, *Phys. Rev. Accel. Beams*, vol. 20, p. 012001, 2017.
- [11] B. Xiao *et al.*, *Phys. Rev. Accel. Beams*, vol. 18, p. 041004 2015.
- [12] S. U. De Silva, J. R. Delayen, *Phys. Rev. Accel. Beams*, vol. 16, p. 082001, 2013.
- [13] A. Lunin *et al.*, in *Proc. LINAC’14*, Geneva, Switzerland, 2014, p. 966.
- [14] Z. Conway *et al.*, in *Proc. IPAC’14*, Dresden, Germany, 2014, p. 2595.
- [15] D. W. Storey, “A Superconducting RF Deflecting Cavity for the ARIEL e-Linac Separator”, Ph.D. Dissertation, Univ. Victoria, Canada, 2018.
- [16] S. Verdu-Andres *et al.*, in *Proc. SRF’13*, Paris, France, 2013, p. 995.
- [17] Z. Li, J. R. Delayen, S. U. De Silva, H. Park, R. Olave, in *Proc. IPAC’15*, Richmond, VA, USA, 2015, p. 3492.
- [18] H. Park, “USLARP Crab Cavity Test Results”, International Review of the Crab Cavity Performance for HiLumi, April 2017.
- [19] S. Verdu-Andres *et al.*, *Phys. Rev. Accel. Beams*, vol. 21, p. 082002, 2018.
- [20] S. Verdu-Andres *et al.*, in *Proc. IPAC’19*, Melbourne, Australia, 2019, p. 3043.
- [21] S. U. De Silva, H. Park, J. R. Delayen, and Z. Li, in *Proc. SRF’17*, Lanzhou, China, 2017, p. 509.
- [22] L. R. Carver *et al.*, in *Proc. IPAC’19*, Melbourne, Australia, 2019, p. 338.
- [23] G. Vandoni *et al.*, in *Proc. SRF’19*, Dresden, Germany, 2019, paper THP106.
- [24] A. Castilla *et al.*, in *Proc. IPAC’17*, Copenhagen, Denmark, 2017, p. 1077.
- [25] T. Capelli *et al.*, in *Proc. SRF’19*, Dresden, Germany, 2019, paper MOP099.
- [26] R. Calaga, “SPS Beam Measurements & Operational Challenges”, International Review of the Crab Cavity for HL-LHC, June 2019.
- [27] J. Mitchell, “HOM Damping and SPS Measurements”, International Review of the Crab Cavity for HL-LHC, June 2019.
- [28] T. Capelli, “RFD Cryomodule Design for SPS Tests”, International Review of the Crab Cavity for HL-LHC, June 2019.
- [29] S. Verdu-Andres, I. Ben-Zvi, Q. Wu, and B. Xiao, in *Proc. SRF’17*, Lanzhou, China, 2017, p. 382.
- [30] H. Park, S. U. De Silva, S. I. Sosa, and J. R. Delayen, in *Proc. IPAC’19*, Melbourne, Australia, 2019, p. 3027.